CrossMark
click for updates

View Article Online
View Journal

Journal of
Materials Chemistry A

Accepted Manuscript

This article can be cited before page numbers have been issued, to do this please use: Y. Xue, P. Guo, H. Yip, Y. Li and Y. CAO, *J. Mater. Chem. A*, 2017, DOI: 10.1039/C6TA09925D.

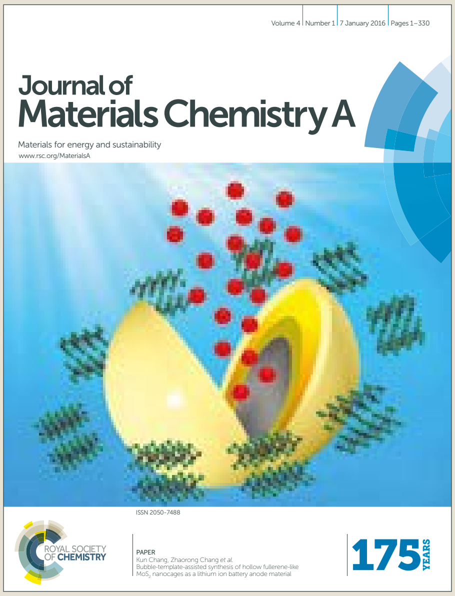

Volume 4 | Number 1 | 7 January 2016 | Pages 1–330

Journal of
Materials Chemistry A

Materials for energy and sustainability
www.rsc.org/MaterialsA

ISSN 2050-7488

ROYAL SOCIETY OF CHEMISTRY

PAPER
Kun Chang, Zhaorong Chang et al.
Bubble-template-assisted synthesis of hollow fullerene-like MoS_2 nanocages as a lithium-ion battery anode material

175 YEARS

This is an Accepted Manuscript, which has been through the Royal Society of Chemistry peer review process and has been accepted for publication.

Accepted Manuscripts are published online shortly after acceptance, before technical editing, formatting and proof reading. Using this free service, authors can make their results available to the community, in citable form, before we publish the edited article. We will replace this Accepted Manuscript with the edited and formatted Advance Article as soon as it is available.

You can find more information about Accepted Manuscripts in the author guidelines.

Please note that technical editing may introduce minor changes to the text and/or graphics, which may alter content. The journal's standard Terms & Conditions and the ethical guidelines, outlined in our author and reviewer resource centre, still apply. In no event shall the Royal Society of Chemistry be held responsible for any errors or omissions in this Accepted Manuscript or any consequences arising from the use of any information it contains.

ROYAL SOCIETY
OF CHEMISTRY

rsc.li/materials-a

View Article Online
DOI: 10.1039/C6TA09925D

Journal Name

COMMUNICATION

General Design of Self-Doped Small Molecules as Efficient Hole Extraction Materials for Polymer Solar Cells

Received 00th January 20xx,
Accepted 00th January 20xx

DOI: 10.1039/x0xx00000x

www.rsc.org/

Yuyuan Xue,[a] Peipei Guo,[b] Hin-Lap Yip,[b,] * Yuan Li[a,] * and Yong Cao[b]

The development of high performance hole transport materials (HTMs) without chemical dopant is critical to achieve long-term device durability. The general design of self-doped materials based on phenolamine structure with strong electronic spin concentration is reported for the first time. The phenol-enhanced self-doped mechanism is also proposed. Comparing with their precursors, demethyl phenolamine derivatives, **TBP-OH4**, **TPD-OH4** and **Spiro-OH8**, displayed much higher spin concentration in their neutral states. Phenol acts as hole trap in traditional concept, however, the films of **TBP-OH4**, **TPD-OH4** and **Spiro-OH8** exhibited higher conductivities than those of methoxyl precursors. Meanwhile, phenolamine derivatives are good soluble in polar organic solvents and show good solvent resistance in chlorobenzene. Considering the relatively good band alignment, film-formation and solvent resistance against chlorobenzene, **Spiro-OH8** and **TPD-OH4** exhibited comparable performance with that of PEDOT:PSS-4083. Most importantly, a new generation of self-doped system based on phenolamine structure might provide new insight to develop efficient HTMs for organic electronics.

Solution-processed polymer solar cells (PSCs) based on bulk heterojunction (BHJ) active layer structure, have gained particular attention because of their potential for low-cost fabrication and high power conversion efficiency (PCE).[1-2] p-Doped and water soluble poly(3,4-ethylenedioxythiophene):poly(styrenesulfonate) (PEDOT: PSS) is the most widely used hole extraction material (HEM) in PSCs due to the high conductivity, anti-erosion and solution processability.[2g-2i] However, indispensable chemical dopant of PSS gives rise to a series of negative effects, like device fabrication and durability.[2a] The manufacturing of high hole-mobility of HEMs without additional chemical dopants, is becoming one of the most critical issues for achieving long-term device durability and practical application.

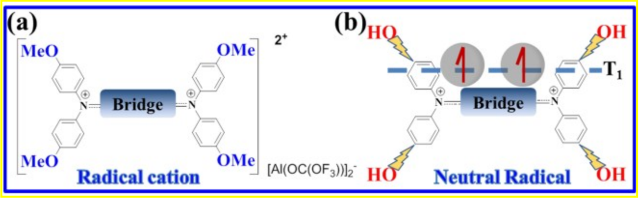

Figure 1. Chemical structure of diadical cation and self-doped triarylamine derivatives.

Herein, a series of polar solvent soluble phenolamine derivatives, **TPA-OH2**, **TBP-OH4**, **TPD-OH4** and **Spiro-OH8**, were obtained by substitution of the -OMe groups on triphenylamine derivatives with -OH groups. The detailed synthetic scheme and characterization of the products were provided in the supporting information (SI) (Scheme S1, Figure S2-S8).[3] Interestingly, a neutral radical system was found in triphenylamine derivatives, namely as self-doped behavior, which was completely different with the traditional radical cation of triarylamines by Wang (Figure 1).[4b, 4e] The radical species and physical property of triphenylamine derivatives were thoroughly studied by cyclic voltammograms (CV), UV-vis-NIR spectra, variable temperature ^{1}H NMR (VT NMR), electron spin resonance spectra (ESR) and hole-only electronic device. It is worth noting that phenolamine derivatives show a much higher spin concentration than those of methoxyl precursors. Comparing with the methoxyl precursors, the strong self-doped behavior of phenolamine derivatives resulted in a higher conductivity. Finally, for the relatively good anti-erosion and film-formation properties, **Spiro-OH8** and

Table 1. Optical, Electrochemical Properties and Energy Level of **TPA-OH2**, **TBP-OH4**, **TPD-OH4** and **Spiro-OH8**

Samples	λ_{abs} (nm)	E_g^{Opt} (eV)	E_{ox}^{onset} (V vs Ag/AgCl)	HOMO (eV)	LUMO (eV)
TPA-OH2	294	3.22	0.59	-5.29	-2.07
TBP-OH4	310	3.02	0.21	-4.91	-1.89
TPD-OH4	296, 350	3.02	0.46	-5.16	-2.14
Spiro-OH8	301, 386	2.93	0.38	-5.08	-2.15

[a.] *School of Chemistry and Chemical Engineering, State Key Laboratory of Pulp and Paper Engineering. South China University of Technology, Guangzhou, China.*
[b.] *Institute of Polymer Optoelectronic Materials and Devices, State Key Laboratory of Luminescent Materials and Devices. South China University of Technology, Guangzhou, China.*
† E-mail: celiy@scut.edu.cn, msangusyip@scut.edu.cn.

View Article Online
DOI: 10.1039/C6TA09925D

TPD-OH4 were applied as HEM in PSCs and their hole extraction property were also studied.

The typical peaks of UV-vis absorption appeared at 294 nm, 310 nm, 350nm and 380 nm for **TPA-OH2**, **TBP-OH4**, **TPD-OH4** and **Spiro-OH8**, respectively (Table 1). Before and after demethylation， the compounds showed relatively similar UV-vis absorption bands and photoluminescence (PL) spectra (Figure S10). It was noteworthy that the color of the products obviously deepened in powder form after demethylation, which was in good agreement with the results of the enlarged UV-vis spectra in the low-energy absorbance of the four products (Figure S11). Considering the molecular structure of the four phenolamine derivatives, their low-energy absorbance might come from the radical state.[4]

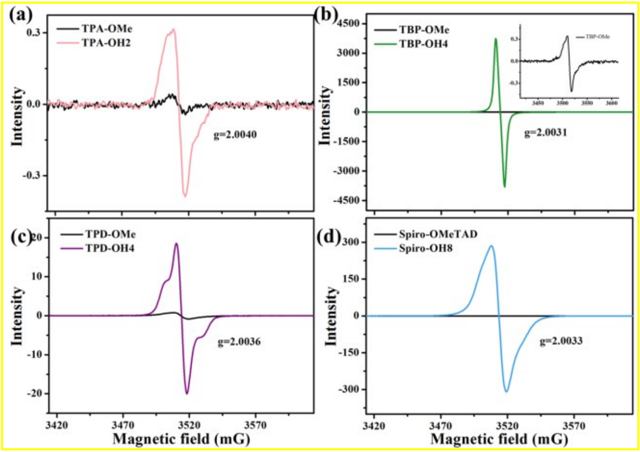

Figure 2. Electron spin resonance (ESR) spectra of solid powders of (a) TPA-OMe and **TPA-OH2**, (b) TBP-OMe and **TBP-OH4**, (c) TPD-OMe and **TPD-OH4**, (d) Spiro-OMeTAD and **Spiro-OH8** at room temperature.

Therewith, ESR experiments were illustrated in Figure 2 to investigate the radical state of the products. The g values of **TPA-OH2**, **TBP-OH4**, **TPD-OH4** and **Spiro-OH8** were 2.040, 2.0031, 2.0036 and 2.0033, respectively, which are very similar with each other. Meanwhile, the spin concentration of the four products significantly increased after the demethylation. Especially, the spin concentration of **TBP-OH4** increased to 10^4 fold than that of TBP-OMe. Meanwhile, the spin concentration of **TPA-OH2**, **TPD-OH4** and **Spiro-OH8** were also estimated to be 8, 24 and 3352 fold, respectively, with the corresponding methoxyl precursors as reference. It is interesting that **TBP-OH4** showed relatively higher spin concentration and no clear hyperfine spectrum could be detected in its ^{1}H NMR result (Figure S5). It is likely that the reason stems from the excited triplet state at room temperature.[4a, 4b, 4d]

Firstly, in order to reveal the origin of radical signal of these neutral compounds, the VT NMR of **TBP-OH4** and its radical cation species was investigated. **TBP-OH4** showed obviously delocalized radical with a relatively broadening ^{1}H NMR signal at room temperature and further broadened at elevated temperatures (Figure 3b). It indicated that the more thermally excited triplet diradical species was generated with the increasing temperature. However, it has been demonstrated that the diradical cation of **TBP-OH4**, which was obtained by adding excess $[NO]^+[PF_6]^-$, was no ^{1}H NMR signal of aromatic protons in CD_3OCD_3 solution with a total triplet state at room temperature (Figure S12). It revealed that the radical species of **TBP-OH4** was not from its diradical cation.

Moreover, the ^{1}H NMR peaks of **TBP-OH4** became obviously sharper, when the temperature decreased to -80 °C, particularly for the protons b and c+d (figure 3). Meanwhile, the decrease of temperature led to downfield shift of the phenolic proton, which can be explained by enhanced intermolecular interaction. This phenomenon of VT NMR would not happened in the molecule of monoradical cation, owing to the S=1/2 state. It indicated that the radical species of **TBP-OH4** was also not from its monoradical cation.

Secondly, **TPA-OH2**, **TBP-OH4**, **TPD-OH4** and **Spiro-OH8** can be readily purified with the mixed solution of petroleum ether and ethyl acetate on the silica gel. It indicated that the whole molecules of **TPA-OH2**, **TBP-OH4**, **TPD-OH4** and **Spiro-OH8** were in the neutral state instead of forming radical cations due to its low polarity (Figure S14). Furthermore, the XPS and element analyses of **Spiro-OH8** also confirmed the neutral state because there was no Br^- anion, which might come from the by-product of the raw material of BBr_3, in its powder form (Table S1 and Figure S13).

Finally, the products with deep color could also be eluted in the thin layer chromatography (TLC) analysis, especially for TBP-OH4, owing to its obviously visible deep green color (Figure S14). It was demonstrated that the low-energy absorbance come from the corresponding radical state. This result further confirmed that the radical species of **TPA-OH2**, **TBP-OH4**, **TPD-OH4** and **Spiro-OH8** were not from their radical cations.

All the three experiments above provided solid evidences for the neutral state of the radical species of the four products. Meanwhile, methoxyl precursors also showed a lower spin concentration comparing with those of phenolamine derivatives (Figure 2 and S15). Furthermore, we also provided another low band-gap triphenylamine derivative, TPA-OMe-DPP, based on 2,5-dihydropyrrolo[3,4-c]pyrrole-1,4-dione (DPP) block and the synthesis, ^{1}H NMR and mass spectrum were provided in SI (Scheme S2, Figure S1, S9 and S15). TPA-OMe-DPP also showed ESR signal in the solid form and ^{1}H NMR signal broadening in aromatic protons in $CDCl_3$ (Figure S15a).

It revealed that the mechanism of radical species above not only existed in phenolamine derivatives but also in methoxyl derivatives. Considering the general radical signal and neutral state of triphenylamine derivatives, we conjectured a radical state existed in pristine triphenylamine derivatives instead of the radical cation (Figure 3a).[4] The proposed mechanism is described as follows. For example, two electrons were excited from the symmetrical phenolamine groups into the LUMO of **TBP-OH4**, respectively, thus leaving two holes in the HOMO of **TBP-OH4**.[5] The symmetrical phenolamine groups still contain one lone electron, respectively, and therefore the holes in the **TBP-OH4** are backfilled by the electron transferred from the symmetrical phenolamine groups. A pair of free electrons remains in the LUMO of **TBP-OH4**, and is stabilized by the quinonoid resonance structure and intermolecular interaction. As a result, the **TBP-OH4** molecule partially exists as excited triplet state at room temperature with an S=1 state.[5] Thus,

View Article Online
DOI: 10.1039/C6TA09925D

the whole molecule of **TBP-OH4** is neutral state. The low-energy absorbance of **TBP-OH4** was from the resonance structure of the connection of two nitrogen radical centers. The other triphenylamine derivatives have the similar mechanism with **TBP-OH4**.

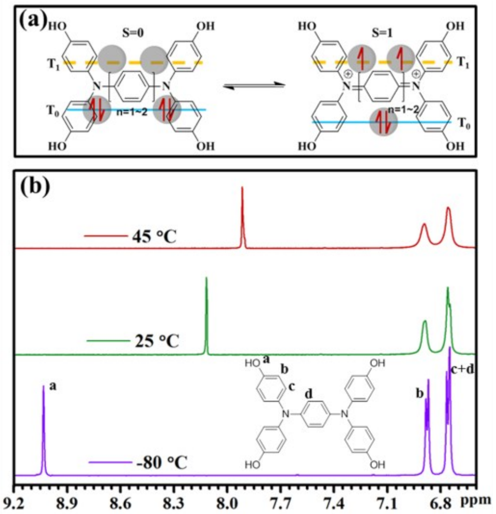

Figure 3. (a) The proposed resonance structure. (b) Variable-temperature ^{1}H NMR spectra of **TBP-OH4** in CD_3COCD_3 and assignment of all aromatic and phenolic protons.

It is worth noting that phenolamine derivatives show a much higher spin concentration than those of their corresponding methoxyl precursors. When the -OMe substituent was replaced by -OH group, oxidation potential of triphenylamine derivatives showed slight decrease (Figure S16). In addition, comparing with the corresponding methoxyl derivatives, the band gap of phenolamine derivatives was obviously narrower in the solid state, resulting in the low-energy absorbance, which was related with their hydrogen bond of phenolamine derivatives in solid state. Thus, with the increased HOMO level and decreased energy band gap, the electron might be excited from the ground state more easily. We conclude that -OH group is beneficial for the generation and stabilization of radical species.

As the discussion above, the easily excited electron from ground state and intermolecular interaction play very important roles in the self-doped system.

In order to further study the radical state of **TPA-OH2**, **TBP-OH4**, **TPD-OH4** and **Spiro-OH8** in their neutral states, the oxidized and charged state of these materials were probed by chemical oxidation (Figure S18). Therefore, considering the CV measurements of the phenolamine derivatives (Figure S16), the nitrosonium hexafluorophosphate $[NO]^+[PF_6]^-$ with a formal potential of 1.4 V, should be an effective oxidant to obtain their radical cations.[4d] **TPA-OH2** could be easily oxidized into a monocation, with two relatively sharp absorptions with λ_{max} at 500 and 747 nm. **TBP-OH4** was oxidized to the monoradical cation by moderate $[NO]^+[PF_6]^-$, with three absorption band over the visible and NIR regions (λ_{max}: 418, 589 and 1014 nm). After adding excess $[NO]^+[PF_6]^-$, the radical cation was further oxidized into diaradical cation (λ_{max}: 515 nm). The -OH group in **TBP-OH4** could not be oxidated with excess $[NO]^+[PF_6]^-$, which was confirmed by ^{1}H NMR (Figure S12). Similarly, **TPD-OH4** could be easily oxidized into monoradical cation (λ_{max}: 493, 719 and 1295 nm), and then diaradical cation (λ_{max}: 498 nm) with excess $[NO]^+[PF_6]^-$. According to the CV data, **Spiro-OH8** undergoes two-electron oxidation to diradical dication with trace $[NO]^+[PF_6]^-$ (a broad absorption between 435 nm and 838 nm; λ_{max}: 1338 nm), and then two-electron oxidation to the tretracation with excess $[NO]^+[PF_6]^-$ (λ_{max}: 522 nm).

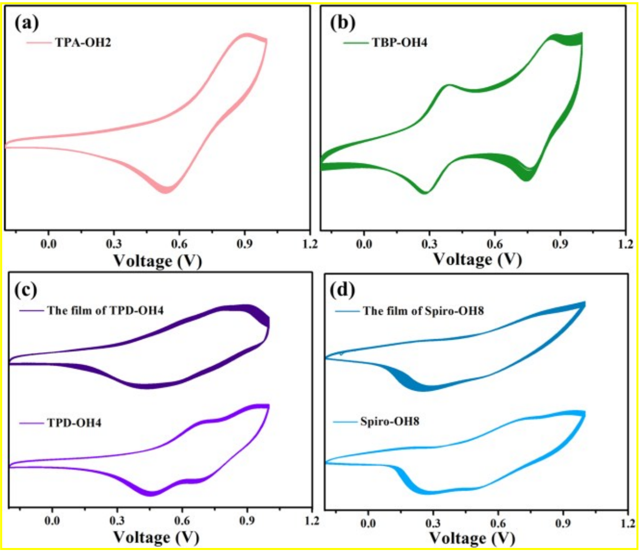

Figure 4. Electrochemical stability experiment of (a) **TPA-OH2**, (b) **TBP-OH4**, (c) **TPD-OH4** and (d) **Spiro-OH8** was performed in CH_2Cl_2/CH_3CN (V_{CH2Cl2}/V_{CH3CN}=250/1) solution at a scan rate of 50 mV/s; the films were spin-coating on ITO.

The electrochemical stability of phenolamine derivatives were also conducted (Figure 4). The CV curves of **TPD-OH4** and **Spiro-OH8** were measured both in solution and film states. Owning to the poor film-formation, the CV results of **TPA-OH2** and **TBP-OH4** were only measured in solution. All of them had the reversible peaks under the oxidative process and showed negative change after 20 repetitive cycles, which was comparable with their corresponding methoxyl precursors (Figure S17). It indicated that phenolamine derivatives showed a good electrochemical stability.

Table 2. The conductivities of Spiro-OMeTAD, TBP-OH4, TPD-OH4 and Spiro-OH8 films[a)]

Samples	Spiro-OMeTAD	TBP-OH4	TPD-OH4	Spiro-OH8
Thickness (nm)	90	60	30	30
Conductivity (S cm^{-1})	6.7×10^{-7}	1.3×10^{-5}	1.0×10^{-5}	3×10^{-6}

[a)] The conductivities of TBP-OMe and TPD-OMe were lower than 10^{-8} S cm^{-1}. TPA-OMe and **TPA-OH2** cannot be detected as their poor film formation property.

The self-doped behavior could greatly enhance the charge transport property of the material.[6] Therefore, the conductivities of TBP-OMe, TPD-OMe, Spiro-OMeTAD, **TBP-OH4**, **TPD-OH4** and **Spiro-OH8** films with no treatment, were measured (Table 2). Due to the poor film formation, the conductivities of TPA-OMe and **TPA-OH2** were not measured. The conductivity of **TBP-OH4**, **TPD-OH4** and **Spiro-OH8** films were 1.3×10^{-5} S cm^{-2}, 1.0×10^{-5} S cm^{-2} and 3.0×10^{-6} S cm^{-2}, respectively. The conductivity of Spiro-OMeTAD film was 6.7 ×

View Article Online
DOI: 10.1039/C6TA09925D

10^{-7} S cm^{-2}. However, the sheet resistances of TBP-OMe and TPD-OMe films were too large and cannot be measured in our test. The obvious increase of conductivity was also one of the solid evidence to prove the self-doped mechanism in phenolamine materials. Moreover, the conductivity of **Spiro-OH8** also had an obvious increase with the increasing annealing temperature in the hole only device, which indicated that the radical state of **Spiro-OH8** could be stimulated by temperature (Figure 5b).

As expected, after demethylation, the four products were highly soluble in DMSO, DMF (> 300 mg/mL), methanol, acetone, and ethyl acetate but insoluble in chloroform, toluene and chlorobenzene, which was contrary to methoxyl-based materials and provided a good orthogonal solvent processibility to contract multilayer devices process from solutions (Figure S22a). Meanwhile, considering the good anti-erosion, film formation and band alignment, **Spiro-OH8** was applied in the PSC devices.

The water contact angle, thermal property and energy level of **Spiro-OH8** were studied before the devices fabrication (Figure S19, S20 and S22). The surface of **Spiro-OH8** (68.7^{o}) is more hydrophobic than that of PEDOT: PSS (57.3^{o}). In addition, the water contact angle of other two materials, **TBP-OH4** (71.4^{o}) and **TPD-OH4** (68.3^{o}), also showed higher hydrophobicity than that of PEDOT: PSS. It revealed that the film of phenolamine derivatives would help to improve the coverage of the active layer as it is typical hydrophobic in nature.[7] Meanwhile, phenolamine derivatives might have a high performance to expel moisture away from the devices. **Spiro-OH8** exhibited a thermal decomposition temperature (T_d) of 371 °C and glass transition temperature (T_g) of 98 °C. The HOMO of **Spiro-OH8** was calculated to be -5.08 eV from CV measurement, which is almost the same with that of PEDOT: PSS (Table 1).[2]

As we know, proper doping is benefit for the performance of Spiro-OMeTAD in PVSC.[8] For the light-induced doping effect on doped Spiro-OMeTAD film, the doping level is not controllable and easily lead to degradation of solar cell device performance.[8b] However, UV-irradiation ESR experiment showed that **Spiro-OH8** powder was very stable under strong UV-irradiation of 100 W (Figure S21).

The performance of **Spiro-OH8** was evaluated by fabricating BHJ polymer solar cells (Table 3, Figure 5 and S25), with a device structure of indium tin oxide (ITO)/HEM/PTB7-Th:$PC_{71}BM$/PFN-Br/Al (Figure 5a and S24), and the detailed PSC preparation is described in Supporting Information (SI). The best **Spiro-OH8** based device exhibited a PCE of 8.20 %, with an open circuit voltage (V_{oc}) of 0.740 V, a short current density (J_{sc}) of 16.51 mA cm^{-2} and a fill factor (*FF*) of 67.1 % by spin-coating **Spiro-OH8** at 5 mg/mL. Meanwhile, in order to further understand the performance of phenolamine derivative in PSCs as HEM, **TPD-OH4** was also employed in devices. The device with **TPD-OH4** as HEM also showed a good performance, yielding the highest PCE of 8.16 % (V_{oc}=0.700 V, J_{sc}=16.97 mA cm^{-2}, *FF*=68.5 %). The PCE of **Spiro-OH8** based device is better than that of **TPD-OH4** based device, which is mainly related to the improved V_{oc}. It is good agreement with the slight difference of HOMO level between **Spiro-OH8** and **TPD-OH4** (Table 1). Moreover, the performances of **Spiro-OH8** and **TPD-OH4** are much higher than that of bare ITO-based devices. The PEDOT: PSS control device showed a relatively better performance, yielding the highest average PCE of 8.40 % (V_{oc}=0.780 V, J_{sc}=15.52 mA cm^{-2}, *FF*=69.5 %).[2d] PEDOT: PSS based devices showed a slightly higher V_{oc} than **Spiro-OH8** and **TPD-OH4** due to the relatively appropriate HOMO level between that of ITO and PTB7-Th. Considering the relatively poor film property in terms of electrical conductivity, **Spiro-OH8** showed a lower *FF* than PEDOT: PSS (Figure S23).[9] Interestingly, comparing the J_{sc} of **Spiro-OH8** with that of PEDOT: PSS, **Spiro-OH8** showed an obvious advantage.

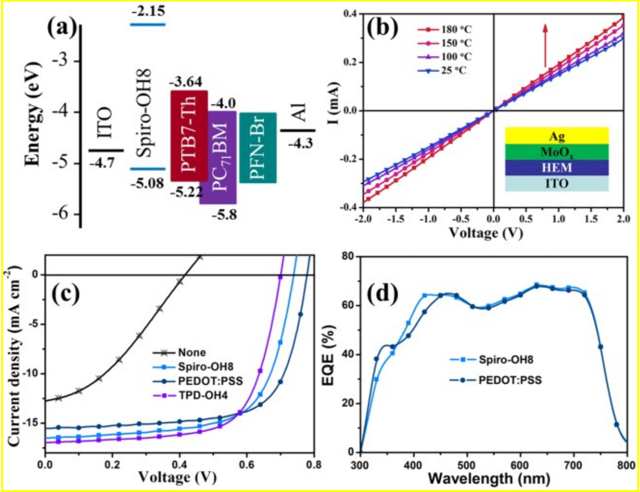

Figure 5. (a) Energy level diagram for each layer in PVS device. (b) *I-V* curves of hole-only devices with different annealing temperature. (c) *J-V* curves of the devices fabricated with none HEM, **Spiro-OH8** (5 mg/mL) and PEDOT: PSS as HEM, respectively; and (d) the corresponding EQE spectra.

Table 3. Photovoltaic parameters for polymer solar cell using with different HEMs

HEM	J_{sc} (mA/cm^2)	V_{oc} (V)	*FF*	PCE (%)
PEDOT: PSS 40nm	15.52	0.780	69.5	8.40
TPD-OH4 5 mg/mL	16.97	0.700	68.5	8.16
Spiro-OH8 5 mg/mL	16.51	0.740	67.1	8.20
Spiro-OH8 10 mg/mL	16.70	0.701	64.8	7.60
Spiro-OH8 16 mg/mL	16.37	0.707	64.5	7.47

Meanwhile, the dependence of device performance on HEM thickness was investigated by spin-coating different concentration **Spiro-OH8** solutions from 5-16 mg/mL. The roughness decreased with the increasing spin-coating concentration of **Spiro-OH8** (Figure S23), however, the performance of the devices declined gradually with increasing HEM thickness. The degradation of the PCEs is mainly due to the decline of V_{oc} and FF, whereas J_{sc} did not change. To understand the high performance of **Spiro-OH8**, the external quantum efficiency (EQE) of the devices was also investigated (Figure 5d and S25b). **Spiro-OH8** showed higher EQE in the 370-450 nm, despite the EQE of **Spiro-OH8** in the 300-370 nm range was lower than that of PEDOT: PSS. In contrast, with the increasing thickness of **Spiro-OH8**, the EQE decreased in the UV absorption range of **Spiro-OH8**, which was in good agreement with *J-V* results and showed similar trends (Figure

View Article Online
DOI: 10.1039/C6TA09925D

S25b). As the whole, **Spiro-OH8** and **TPD-OH4** exhibited comparable performance with that of PEDOT:PSS-4083.

Finally, the shelf-life stability of PSC devices with self-doped materials as HTMs, was also studied. The devices based on **Spiro-OH8** and **TPD-OH4** presented enhanced stability than that based on PEDOT:PSS-4083 after 216 h of storage. The PCEs based on **Spiro-OH8** and **TPD-OH4** droped 16.5% (Figure S26) and 17.3% after 216 h, respectively, comparing with 24.2% of PEDOT:PSS (Figure 6). The decrease of the PSCs performance was attributed to the parameters of *FF* and J_{sc}.

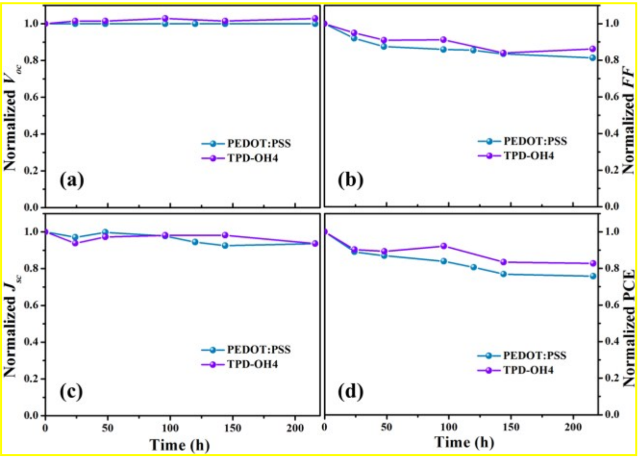

Figure 6. Time-course variation of the photovoltaic parameters of **TPD-OH4** and PEDOT:PSS-4083 based polymer solar cells, storing in nitrogen protected glove box without encapsulation. a) Normalized V_{oc}, b) Normalized *FF*, c) Normalized J_{sc}, d) Normalized PCE.

Conclusions

In summary, a novel phenolamine based neutral radical system with high spin concentration, was found for the first time and its self-doped mechanism was proposed. Phenolamine structure is beneficial for the generation and stabilization of radical species, owning to the strong intermolecular interaction and electron-donating effect. Self-doped **Spiro-OH8** was successfully applied as HEM in polymer BHJ solar cells, showing PCE values up to 8.20%. This is an encouraging result as the performance is comparable to that based on commercial PEDOT: PSS material. Phenolamine structure is an efficient building block to achieve high-efficient HEM. Meanwhile, the activation of phenolamine structure induced the radical state with an enhanced conductivity. This new design strategy might provide a new access to develop novel and efficient semiconductors for organic electronics.

Acknowledgements

The authors would like to acknowledge the financial support of the National Natural Science Foundation of China (21402054, 21436004), the Ministry of Science and Technology (2014CB643501, 2014CB643505) and the Natural Science Foundation of China (51323003, 51273069, 51573057).

Notes and references

1 (a) H. Bin, L. Gao, Z. G. Zhang, Y. Yang, Y. Zhang, C. Zhang, S. Chen, L. Xue, C. Yang, M. Xiao and Y. Li, *Nat. Commun.*, 2016, **7**, 13651; (b) Z. Li, K. Jiang, G. Yang, J. Y. L. Lai, T. Ma, J. Zhao, W. Ma and H. Yan, *Nat. Commun.*, 2016, **7**, 13094; (c) H. L. Yip and A. K. Y. Jen, *Energ. Environ. Sci.*, 2012, **5**, 5994; (d) C. Duan, K. Zhang, C. Zhong, F. Huang and Y. Cao, *Chem. Soc. Rev.*, 2013, **42**, 9071; (e) G. H. Jun, S. H. Jin, B. Lee, B. H. Kim, W. S. Chae, S. H. Hong and S. Jeon, *Energ. Environ. Sci.*, 2013, **6**, 3000; (f) V. Vohra, K. Kawashima, T. Kakara, T. Koganezawa, I. Osaka, K. Takimiya and H. Murata, *Nat. Photonics*, 2015, **9**, 403; (g) Y. M. Yang, W. Chen, L. Dou, W. H. Chang, H. S. Duan, B. Bob, G. Li and Y. Yang, *Nature Photonics,* 2015, **9**, 190.

2 (a) M. P. De Jong, L. J. Van Ijzendoorn and M. J. A. De Voigt, *Appl. Phys. Lett.*, 2000, **77**, 2255; (b) R. Po, C.,Carbonera, A. Bernardi and N. Camaioni, *Energ. Environ. Sci.*, 2011, **4**, 285; (c) H. Q. Zhou, Y. Zhang, C. K. Mai, S. D. Collins, T. Q. Nguyen, G. C. Bazan and A. J. Heeger, *Adv. Mater.*, 2014, **26**, 780; (d) Z. He, B. Xiao, F. Liu, H. Wu, Y. Yang, S. Xiao, C. Wang, T. P. Russell and Y. Cao, *Nat. Photonics*, 2015, **9**, 174; (e) W. Zhao, D. Qian, S. Zhang, S. Li, O. Inganäs, F. Gao and J. Hou, *Adv. Mater.*, 2016, **28**, 4734; (f) L. Nian, K. Gao, F. Liu, Y. Kan, X. Jiang, L. Liu, Z. Xie, X. Peng, T. P. Russell and Y. Ma, *Adv. Mater.*, 2016, **28**, 8184; (g) Y. Li and N. L. Hong, *J. Mater. Chem. A*, 2015, **3**, 21537; (h) Y. Wu, J. Wang, X. Qiu, R. Yang, H. Lou, X. Bao and Y. Li, *ACS Appl. Mater. Inter.*, 2016, **8**, 12377; (i) Y. Li, M. Liu, Y. Li, Y. K., L. Xu, W. Yu, R. Chen, X. Qiu and H. L. Yip, *Adv. Energy Mater.,* DOI: 10.1002/aenm.201601499.

3 (a) B. Kamino, B. Mills, C. Reali, M. Gretton, M. Brook and T. Bender, *J. Org. Chem.*, 2012, **77**, 1663; (b) J. Lee, K. Baek, M. Kim, G. Yun, Y. Ko, N. S. Lee, L. Hwang, J. Kim, R. Natarajan, C. Park, W. Sung and K. Kim, *Nat. Chem.*, 2014, **6**, 97.

4 (a) Y. Li, W. K. Heng, B. S. Lee, N. Aratani, J. L. Zafra, N. Bao, R. Lee, Y. M. Sung, Z. Sun, K. W. Huang, R. D. Webster, J. T. L. Navarrete, D. Kim, A. Osuka, J. Casado, J. Ding and J. Wu, *J. Am. Chem. Soc.*, 2012, **134**, 14913; b) Y. Su, X. Wang, X. Zheng, Z. Zhang, Y. Song, Y. Sui, Y. Li and X. Wang, *Angew. Chem. Int. Edit.*, 2014, **53**, 2857; (c) Y. Li, Y. Xue, L. Xia, L. Hou and X. Qiu, *Phys. Status. Solidi. A*, 2015, **213**, 429; (d) Y. Wang, H. Zhang, M. Pink, A. Olankitwanit, S. Rajca and A. Rajca, *J. Am. Chem. Soc.*, DOI: 10.1021/jacs.6b01498; (e) T. Li, G. Tan, D. Shao, J. Li, Z. Zhang, Y. Song, Y. Sui, S. Chen, Y. Fang and X. Wang, *J. Am. Chem. Soc.*, 2016, **138**, 10092.

5 (a) Z. Wu, C. Sun, S. Dong, X. F. Jiang, S. Wu, H. Wu, H. L. Yip, F. Huang and Y. Cao, *J. Am. Chem. Soc.*, 2016, **138**, 2004; (b) H. Liu, L. Huang, X. Cheng, A. Hu, H. Xu, L. Chen and Y. Chen, *ACS Appl. Mater. Inter.*, DOI: 10.1021/acsami.6b15678.

6 (a) A. G. MacDiarmid, *Angew. Chem. Int. Edit.*, 2001, **40**, 2581; (b) K. Walzer, B. Maennig, M. Pfeiffer and Leo, K. *Chem. Rev.*, 2007, **107**, 1233; (c) W. H. Nguyen, C. D. Bailie, E. L. Unger and M. D. McGehee, *J. Am. Chem. Soc.*, 2014, **136**, 10996.

7 Q. Xue, G. Chen, M. Liu, J. Xiao, Z. Chen, Z. Hu, X. F. Jang, B. Zhang, F. Huang, W. Yang, H. L. Yip and Y. Cao, *Adv. Energy Mater.*, 2016, **6**, 1502021.

8 (a) M. Franckevičius, A. Mishra, F. Kreuzer, J. Luo, S. M. Zakeeruddin and M. Grätzel, *Mater. Horiz.*, 2015, **2**, 613; (b) Y. K. Wang, Z. C. Yuan, G. Z. Shi, Y. X. Li, Q. Li, F. Hui, B. Q. Sun, Z. Q. Jiang and L. S. Liao, *Adv. Funct. Mater.*, 2016, **26**, 1375; (c) C. Yi, J. Luo, S. Meloni, A. Boziki, N. Ashari-Astani, C. Grätzel, S. M. Zakeeruddin, U. Rőthlisberger and M. Grätzel, *Energ. Environ. Sci.*, 2016, **9**, 656.

9 L. Xia, Y. Xue, K. Xiong, C. Cai, Z. Peng, Y. Wu, Y. Li, J. Miao, D. Chen, Z. Hu, J. Wang, X. Peng, Y. Mo and L. Hou, *ACS Appl. Mater. Inter.*, 2015, **7**, 26405.

View Article Online
DOI: 10.1039/C6TA09925D

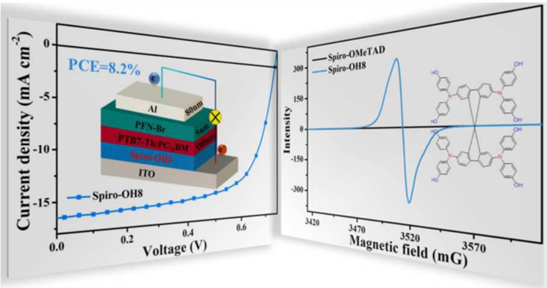

The design of self-doped materials as efficient hole extraction materials for polymer solar cells is reported for the first time.